

Aptamers Switch on Fluorescence of Triphenylmethane Dyes

Jeremy R. Babendure, Stephen R. Adams, and Roger Y. Tsien*

Department of Pharmacology, Howard Hughes Medical Institute, and Biomedical Sciences Program,
University of California, San Diego, La Jolla, California 92093-0647

Received August 18, 2003; E-mail: rtsien@ucd.edu

Fluorescent reporters have revolutionized the study of biological systems by allowing exquisitely sensitive, real-time detection of tagged proteins both in vitro and in vivo. Ideally, the requisite tagging is performed in situ by genetic fusion, either to unusual fluorescent proteins from jellyfish or coral or to much shorter tetracycline domains, which bind and enhance the fluorescence of membrane-permeant biarsenical dyes.¹ However, comparable methods do not yet exist for nucleic acids. No sequence of natural, genetically encodable nucleotides is known to generate distinctive fluorescence by itself. Current methods for visualizing specific nucleotide sequences usually require hybridization to a synthetically labeled complementary probe.² Such hybridization is destructive and incompatible with live cells because of the need to introduce labeled antisense sequences and then stringently wash away the excess of unbound probe. The only way at present to image specific RNAs in a live cell is to fuse such RNAs to tandem multimers of special stem-loop sequences, which attract unique binding proteins that in turn are fused to green fluorescent proteins.³ This tagging system is indirect and adds tremendous mass, around 270 kDa, far larger than the typical RNA target to be tracked. A more compact strategy for genetically tagging RNAs in situ would be to fuse them to the shortest possible nucleotide sequences that can bind specific membrane-permeant dyes and render the latter fluorescent. General methods are now available for selective evolution of oligonucleotides (“aptamers”) that bind small molecules.⁴ An RNA aptamer was evolved to bind malachite green (MG)⁵ in the hope that illumination of the dye would generate reactive oxygen species⁶ to inactivate an attached mRNA.⁷ This MG aptamer was later found to prefer rigidly planar analogues such as tetramethylrosamine (TMR, $K_d \approx 40$ nM) and pyronin Y ($K_d \approx 225$ nM) over nonplanar, rotationally mobile MG (800 nM). Therefore, the crystal structure was determined with TMR instead of MG.⁸ The TMR was embedded between a base quadruple and base pair and suggested that ligand binding was stabilized by base-stacking interactions. In addition, noncanonical base pairs further stabilized the aptamer and encouraged the specificity for TMR.⁸

Triphenylmethane dyes such as MG normally have extremely low quantum yields for fluorescence due to easy vibrational de-excitation, but viscous or cold environments are known to encourage some fluorescence by restricting such vibrations.⁹ We hoped the MG aptamer might do the same and stabilize MG in a planar, more fluorescent conformation. We now show that the MG aptamer indeed increases the fluorescence of MG and close relatives ~2360-fold while rejecting triphenylmethane dyes bearing additional sulfonate groups. Conversely, another aptamer raised against a sulfonated rhodamine⁷ binds and enhances the fluorescence of sulfonated triphenylmethane dyes while rejecting purely cationic triphenylmethanes such as MG. To our knowledge, these are the first demonstrations of short RNA sequences that can specifically enhance the fluorescence of appropriate dye partners while both crossed combinations are rejected.

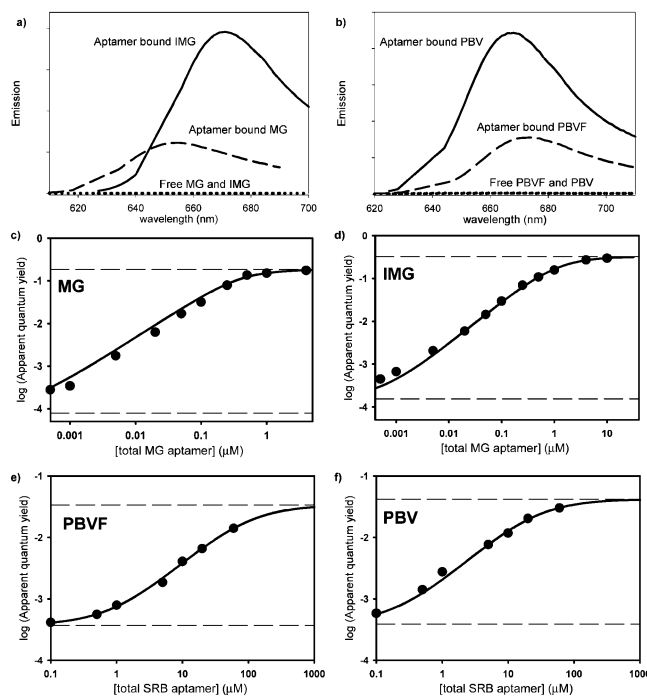


Figure 1. MG and SRB aptamers enhance fluorescence of triphenylmethane dyes. (a) Emission spectra of IMG and MG with and without excess MG aptamer. (b) Emission spectra of PBVF and PBV with and without 60 μ M SRB aptamer. (c–f) Apparent quantum yields for MG, IMG, PBVF, and PBV as a function of total aptamers. Solid circles are experimental, and smooth curves are the best fits for 1:1 binding (see Supporting Information). Lower and upper asymptotes indicate the measured quantum yield for free dye and the fitted quantum yield for the complex.

Free MG in 100 mM KCl, 5 mM $MgCl_2$, and 10 mM HEPES (pH 7.4) had an absorbance maximum at 618 nm and very low fluorescence, corresponding to a quantum yield of 7.9×10^{-5} . MG aptamer RNA⁸ was transcribed from a DNA template containing a double-stranded T7 promoter region and was gel purified. RNA (4 μ M) was folded into MG aptamers in the above buffer and mixed with 0.32 μ M MG. The aptamer shifted the MG absorbance from 618 to 630 nm, consistent with previous reports,⁵ indicating that the MG was nearly fully bound. Titration with increasing amounts of MG aptamer and curve-fitting the fluorescence to an equation for 1:1 complexation yielded a dissociation constant of 117 nM (Figure 1c). This value indicates somewhat stronger binding than the 800 nM K_d previously reported,⁸ which was indirectly determined at pH 5.8 in a low ionic-strength medium by MG competition with TMR binding. The fluorescence of the aptamer-bound MG (Figure 1a,c) was tremendously enhanced to a quantum yield of 0.187 in the limit of 100% binding, 2360 times greater than that of unbound MG (Table 1). This quantum yield for the MG aptamer complex exceeds those observed when MG and comparable triphenylmethane dyes are adsorbed to albumin or immobilized in

Aptamers Switch On Fluorescence of Triphenylmethane Dyes

Jeremy R. Babendure, Stephen R. Adams, and Roger Y. Tsien

Supplemental Material

Patent Blue dyes PBV and PBVF were purified by HPLC using a C₁₈-reverse-phase column with a linear gradient of 10-90% acetonitrile in water with 0.1% TFA. The major peak was collected, evaporated and identified by ES-MS.

Synthesis of IMG:

5,5'-Bis(N-methylindolinyl)phenylmethane:

A solution of N-methyl indoline¹ (133 mg, 1 mmol) and benzaldehyde (51 μ L, 0.5 mmol) in dry CH₂Cl₂ (1 mL) under N₂ at 0 °C was treated with freshly-sublimed AlCl₃ (67 mg, 0.5 mmol). The reaction mixture turned green slowly and was allowed to warm up to room temperature and left overnight. The reaction mixture was quenched with 1M KOH (10 mL) and extracted with CH₂Cl₂ (3 x 15 mL). The extracts were dried over Na₂SO₄ and evaporated to an oil that was purified by SiO₂ chromatography by elution with ethyl acetate-hexanes (1:9 v/v) to give the product as a colorless oil. Yield, 90.8 mg (51%). NMR (¹H, CDCl₃) 2.75 (s, 6H, N-Me), 2.89 (t, 4H, H-2, 2' J=8 Hz), 3.31 (t, 4H, H-3, 3' J=8 Hz), 5.35 (s, 1H, H-1, 1'), 6.45 (d, 2H, H-7, 7' J=7.8 Hz), 6.82 (broad d, 4H, H-4,4',6,6' J=9.4Hz), 7.1-7.3 (m, 5H, phenyl).⁽¹⁾

IMG (bis(N-methylindolinyl) Malachite Green:

5,5'-Bis(N-methylindolinyl)phenylmethane (45mg, 0.13 mmol) dissolved in 2 mL 95% EtOH was treated with chloranil (38 mg, 0.15 mmol) and gently heated until reaction was complete as judged by TLC (SiO₂, 20% MeOH-CHCl₃), in which the product is a green-colored spot with R_f ~0.20). The reaction mixture was evaporated, dissolved in MeOH (1 mL) and 1M-HCl (0.5 mL), heated briefly and re-evaporated. The product was purified by SiO₂ chromatography (eluted with 20% MeOH-CHCl₃) to give a dark green solid. Yield >95%. NMR (¹H-NMR, CDCl₃) 3.20 (s, 6H, N-Me), 3.73 (t, 4H, H-2,2'), 3.94 (t, 2H, H-3,3'), 6.67 (d, 2H, H-7,7'), 7.0 (broad d, 2H, H-6,6'), 7.1-7.6 (broad m, 6H, H-7,7', phenyl).

Synthesis of MG and SRB RNA Aptamers:

Malachite Green aptamer RNA (5' GGAUCCCGA CUGGCGAGAG CCAGGUAACG AAUGGAUCC) and Sulforhodamine B aptamer RNA (5' GGAACCUCGCUUCGGCGAUGAUGGAGAGGCGCAAGGUUAACCGCCUCAGG UUC) were produced as follows: 200 pmol DNA anti-sense to MG aptamer (GGATCCATTCGTTACCTGGCTCTCGCC AGTCGGGATCCTATAGTGAGTCGTATTAAGCT) or SRB aptamer (GGAACCTGAGGCGGTAAACCTTGCGCCTCTCCATCATCGCCGAAGCGAGGTT CCTATAGTGAGTCGTATTAAGCT) were annealed with 200 pmol T7 sense DNA (AGCTTAATACGACTCACTATAGGA) in 200 μ L annealing buffer (50mM NaCl,

100mM HEPES pH7.4). 30 μ L (60pmol) of annealed DNA, 10 μ L (400units) of Invitrogen RnaseOut and 25 μ L (500units) of Promega RNA polymerase was added to a final volume of 500 μ L in transcription reaction buffer (20mM NaCl, 12mM MgCl₂, 4mM spermidine, 20mM DTT, 2mM NTPs and 80mM Tris-HCl pH 7.9). Transcription was allowed to go overnight at 37C. The RNA product was precipitated with ammonium acetate, re-dissolved in formamide gel running buffer and purified by electrophoresis on a 10% denaturing acrylamide gel. RNA aptamers were excised from gel and soaked in dissociation buffer (0.1mM EDTA, 0.1% SDS, 500mM NaCl, 10mM Tris pH7.4). RNA was next ethanol precipitated and dissolved in DEPC treated H₂O. Samples were stored at -20C until further use.

Determination of fluorescence quantum yields and affinities:

All quantum yields were determined by comparing the integral of the corrected emission spectra with the corresponding integral obtained from a solution of Cresyl Violet in methanol, whose absorbance was adjusted to match that of the sample of interest at the excitation wavelength. The absolute quantum yield of Cresyl Violet was taken to be 0.545⁽²⁾. The refractive index correction was negligible because methanol and aqueous buffers differ in refractive index by <0.01.

The quantum yields of the free dyes (Q_D) were determined in 1X selection buffer. Dissociation constants K and quantum yields for their complexes with aptamers (Q_{RD}) were determined by measuring the apparent quantum yields (Q_{app}) as a function of increasing total added RNA (R_T) at a fixed concentration of total dye (D_T), and least-squares fitting to the following model for 1:1 complexation. Let $[R]$ and $[D]$ be the concentrations of free RNA and free dye respectively. Let K be the dissociation constant for their complex. Then the concentration $[RD]$ of the RNA:dye complex is given by:

$$[RD] = \frac{[R][D]}{K} = \frac{(R_T - [RD])(D_T - [RD])}{K}$$

The solution of this quadratic equation for $[RD]$ is

$$[RD] = \frac{D_T + R_T + K - \sqrt{(D_T + R_T + K)^2 - 4D_T R_T}}{2}$$

The apparent quantum yield Q_{app} for a mixture of free dye (whose quantum yield is Q_D) and aptamer-dye complex (whose quantum yield is Q_{RD}) is

$$Q_{app} = \frac{Q_D[D] + Q_{RD}[RD]}{D_T} = Q_D + \frac{(Q_{RD} - Q_D)[RD]}{D_T}$$

$$= Q_D + (Q_{RD} - Q_D) \left[\frac{D_T + R_T + K - \sqrt{(D_T + R_T + K)^2 - 4D_T R_T}}{2D_T} \right]$$

The smooth curves in Fig. 1c-1f are the best fits of the measured R_T and Q_{app} values (solid circles) to the above equation, with K and Q_{RD} as the fitted parameters listed in the text and in Table 1. The measured Q_D and the deduced Q_{RD} are also respectively shown as the lower and upper horizontal asymptotes in Figs. 1c-1f. Total dye concentrations (D_T) were 320 nM for MG (Fig. 1a and 1c), 260 nM for IMG (Fig. 1a and 1d), 1.45 μ M for PBVF (Fig. 1b and 1e), and 1.0 μ M for PBV (Fig. 1b and 1f). For the spectra of aptamer-

dye complexes in Fig. 1a, the concentrations of MG aptamer were 4 μM and 10 μM for MG and IMG respectively. In Fig. 1b, the SRB aptamer was 60 μM for both complexes.

Multimer Data:

To determine if multiplying aptamer sequences in tandem could increase fluorescence intensity levels, we cloned, amplified and transcribed MG aptamer sequences as monomers, dimers, trimers, tetramers and pentamers and compared fluorescence intensity levels at equimolar concentrations of RNA (10 μM). As shown in Fig. 2, increasing the number of concatenated MG aptamers resulted in increased levels of fluorescence, particularly addition of the 3rd and 5th units, whereas the 2nd and 4th units gave lesser increments, suggesting that they may function only as spacers. Currently only 6 bases separate each aptamer unit, so increasing the spacer length might permit each aptamer to fold and bind MG independently, thus increasing fluorescence levels. Nevertheless, these results suggest that multiple MGs bound to concatenated aptamers do not quench each other as multiple fluorophores often do when conjugated to a single antibody. Therefore increased brightness is attainable if higher molecular weight is tolerable.

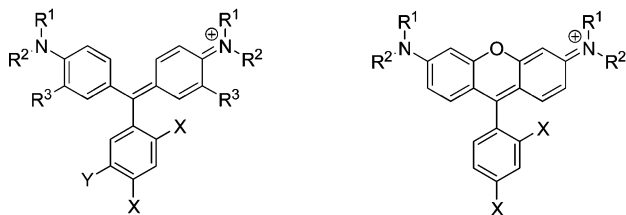


Reference List

- (1) Gribble, G. W.; Nutaitis, C. F. *Synthesis* **1987**, 709-711.
- (2) Magde, D.; Brannon, J. H.; Cremers, T. L.; Olmsted, J. *J.Phys.Chem.* **1979**, 83, 696-699.

Table 1. Spectral Enhancements of Triphenylmethane Dyes Bound to MG and SRB Aptamers

dye	RNA aptamer	$\Delta\lambda_{\max}$ (nm)	QY free	QY bound	fold increase	K_d μM
MG	MG	12	7.9×10^{-5}	0.187	2360	0.117
IMG	MG	8	1.5×10^{-4}	0.324	2090	0.666
PBVVF	SRB	7.5	3.7×10^{-4}	0.034	92	86
PBV	SRB	10	3.9×10^{-4}	0.042	107	23

Chart 1. Relevant Triphenylmethane and Xanthene Dyes

MG: $R^1 = R^2 = \text{Me}$; $R^3 = X = Y = \text{H}$
 IMG: $R^1 = \text{Me}$; $R^2, R^3 = \text{CH}_2\text{CH}_2$; $X = Y = \text{H}$
 PBVVF: $R^1 = R^2 = \text{Et}$, $R^3 = Y = \text{H}$; $X = \text{SO}_3^-$
 PBV: $R^1 = R^2 = \text{Et}$, $R^3 = \text{H}$; $X = \text{SO}_3^-$; $Y = \text{OH}$

TMR: $R^1 = R^2 = \text{Me}$; $X = \text{H}$
 SRB: $R^1 = R^2 = \text{Et}$; $X = \text{SO}_3^-$

glycerol or a sucrose octaacetate glass.⁹ To show that enhancement is specific for the MG aptamer, we added 60 μM sulforhodamine B aptamer RNA (SRB), a different aptamer selected to bind the disulfonated rhodamine dye sulforhodamine B.⁷ This saturating amount of SRB aptamer enhanced MG only slightly. Presumably, the binding cavity of the MG aptamer locks the rotationally mobile MG in a rigid, planar configuration somewhat similar to the planar structure of TMR, whereas the SRB aptamer does not bind MG significantly.

The major nonplanarity and vibrational flexibility in MG is due to the propeller-like twisting of the phenyl rings with respect to the central triarylmethyl carbon, but twisting of the dimethylamino groups relative to the phenyl rings could contribute an additional mode of excited-state deactivation. We therefore rigidized the dialkylamino substituents by synthesizing IMG, an indolinyl derivative of MG (Chart 1). Free IMG showed an absorbance maximum of 642 nm, slightly red-shifted from that of MG, and a quantum yield of 1.55×10^{-4} , about double that of MG (Table 1). Addition of 10 μM MG RNA aptamer to 0.5 μM IMG shifted the absorbance to 650 nm and increased the peak extinction somewhat (Figure 1b). Similar to MG, the fluorescence quantum yield for fully bound IMG was determined to be 0.324 (Table 1). Therefore, rigidization of the dialkylamino substituents increased the quantum yield of both the free and bound dye by about 2 to 3-fold, leaving the enhancement factor near 2090-fold. Titration of fluorescence vs aptamer concentration and curve fit analysis (Figure 1d) indicated a dissociation constant of 666 nM. The weaker affinity for IMG is expected because the MG aptamer was not optimized to bind this analogue. Aptamers selected for IMG itself might be even more effective at increasing its quantum yield. As with MG, 60 μM SRB aptamer had virtually no effect on fluorescence of IMG.

Although the SRB aptamer does not significantly bind or enhance the fluorescence of MG or IMG, are there other dyes whose fluorescence the SRB aptamer can increase? We tested it with the triphenylmethane analogue of sulforhodamine B, patent blue VF (PBVVF). Free PBVVF showed a quantum yield of 3.7×10^{-4} . Addition of 60 μM SRB aptamer caused a bathochromic shift of 7.5 nm and a large fluorescence enhancement (Figure 1b). Curve fitting of fluorescence as a function of SRB aptamer concentration (Figure 1e) yielded a dissociation constant of 86 μM and a quantum yield for the complex of 0.034, an enhancement of 92-fold. We also tested patent blue violet (PBV), an analogue of PBVVF bearing

an extra -OH on the phthalein ring (Chart 1). Free PBV showed a quantum yield of 3.9×10^{-4} . Interestingly, 60 μM SRB aptamer shifted the absorbance of PBV by 10 nm to the red and enhanced PBV fluorescence about twice as much as that of PBVVF (Figure 1b). Curve fitting of titrations yielded a dissociation constant of 23 μM and a quantum yield of 0.042 for the PBV-SRB aptamer complex, a 107-fold enhancement over that for free PBV (Figure 1f). The extra hydroxyl group of PBV therefore almost quadruples the affinity for the aptamer. An aptamer evolved to bind PBV itself might achieve higher affinities and quantum yields closer to those of MG and IMG complexed to the MG aptamer. Addition of 10 μM MG aptamer to both PBVVF and PBV did not cause any fluorescence enhancement, proving that both the MG and SRB aptamers discriminate against the other's ligands.

The ability of aptamers consisting of just 38–54 nucleotides to enhance the fluorescence of specific triphenylmethane dyes up to 2300-fold opens many interesting possibilities for assaying the formation, location, or breakdown of RNAs incorporating such aptamers. In addition, we were able to further enhance fluorescence by cloning and transcribing MG aptamer sequences in tandem, revealing concatenated aptamers result in increased levels of fluorescence without quenching one other (Supporting Information). The specificity of the MG and SRB aptamers for different sets of dyes suggests that it should be possible to discriminate multiple RNAs simultaneously. Because neither aptamer was selected or optimized for the ability to enhance fluorescence, further improvements should be possible. We hope that such progress will enable in situ fluorescent tagging and imaging of important messenger, ribosomal, and micro RNAs to help answer the many biological questions about their metabolism, trafficking, and functions within living cells.

Acknowledgment. We thank Jennie Bever for reviewing the manuscript and Drs. C. Wilson, J. Wang, and J. Ding for helpful suggestions. Supported by HHMI, NIH27177, DOE DE-FG03-01ER63276.

Supporting Information Available: Purification of patent blue dyes, synthesis of IMG, synthesis of aptamer RNA, curve fit analysis and quantum yield determination (PDF). This material is available free of charge via the Internet at <http://pubs.acs.org>.

References

- (1) (a) Zhang, J.; Campbell, R. E.; Ting, A. Y.; Tsien, R. Y. *Nat. Rev. Mol. Cell Biol.* **2002**, *3*, 906–918. (b) Tsien, R. Y. *Annu. Rev. Biochem.* **1998**, *67*, 509–544. (c) Chalfie, M.; Tu, Y.; Euskirchen, G.; Ward, W. W.; Prasher, D. C. *Science* **1994**, *263*, 802–805. (d) Adams, S. R.; Campbell, R. E.; Gross, L. A.; Martin, B. R.; Walkup, G. K.; Yao, Y.; Llopis, J.; Tsien, R. Y. *J. Am. Chem. Soc.* **2002**, *124*, 6063–6076.
- (2) Long, R. M.; Elliott, D. J.; Stutz, F.; Rosbash, M.; Singer, R. H. *RNA* **1995**, *1*, 1071–1078.
- (3) (a) Bertrand, E.; Chartrand, P.; Schaefer, M.; Shenoy, S. M.; Singer, R. H.; Long, R. M. *Mol. Cell* **1998**, *2*, 437–445. (b) Long, R. M.; Gu, W.; Lorimer, E.; Singer, R. H.; Chartrand, P. *EMBO J.* **2000**, *19*, 6592–6601. (c) Irie, K.; Tadauchi, T.; Takizawa, P. A.; Vale, R. D.; Matsumoto, K.; Herskowitz, I. *EMBO J.* **2002**, *21*, 1158–1167.
- (4) (a) Hermann, T.; Patel, D. J. *Science* **2000**, *287*, 820–825. (b) Famulok, M. *Curr. Opin. Struct. Biol.* **1999**, *9*, 324–329.
- (5) Grate, D.; Wilson, C. *Proc. Natl. Acad. Sci. U.S.A.* **1999**, *96*, 6131–6136.
- (6) Jay, D. G.; Keshishian, H. *Nature* **1990**, *348*, 548–550.
- (7) (a) Holeman, L. A.; Robinson, S. L.; Szostak, J. W.; Wilson, C. *Folding Des.* **1998**, *3*, 423–431. (b) Grate, D.; Wilson, C. *Bioorg. Med. Chem.* **2001**, *9*, 2565–2570.
- (8) Baugh, C.; Grate, D.; Wilson, C. *J. Mol. Biol.* **2000**, *301*, 117–128.
- (9) (a) Oster, G.; Nishijima, Y. *J. Am. Chem. Soc.* **1956**, *78*, 1581–1584. (b) Baptista, S. B.; Indig, G. L. *J. Phys. Chem. B* **1998**, *102*, 4678–4688.

JA037994O